

## Characterization and topical delivery of phenylethyl resorcinol

Y. Zhang\*, B. C. Sil†, C.-P. Kung\*, J. Hadgraft\*, M. Heinrich\*, B. Sinko‡ and M. E. Lane\*

\*UCL School of Pharmacy, 29-39 Brunswick Square, London, WC1N 1AX, UK, †London Metropolitan University, 166-220 Holloway Road, London N7 8DB, UK and ‡Pion Inc., 10 Cook Street, Billerica MA, 01821, USA

### ABSTRACT

#### OBJECTIVE:

Phenylethyl resorcinol (PR) has been used widely in the personal care industry as a novel skin lightening ingredient. Surprisingly, there is only limited information describing the physicochemical properties of this active. Therefore, the primary objective of this study was to perform a comprehensive characterization of PR. A secondary objective was to investigate the delivery of this molecule to mammalian skin.

#### METHODS:

PR was characterised using Differential Scanning Calorimetry (DSC), Thermogravimetric Analysis (TGA), and Nuclear Magnetic Resonance (NMR). A new high-performance liquid chromatographic (HPLC) method for analysis of PR was developed and validated. The logP (octanol water partition coefficient), value, solubility and short-term stability of PR in a series of vehicles were also determined using HPLC. The evaporation of the selected vehicles was examined using Dynamic Vapour Sorption (DVS). The permeation profiles of PR were investigated under finite dose conditions in porcine and human skin.

#### RESULTS:

The melting point of PR was determined to be 79.13 ° C and the measured logP (octanol water partition coefficient) at 21 ° C was  $3.35 \pm 0.03$ . The linearity of the HPLC analytical method was confirmed with an  $r^2$  value of 0.99. Accuracy of the method was evaluated by average recovery rates at three tested concentrations, and the values ranged from 99 - 106%. The limit of detection (LOD) and limit of quantification (LOQ) were 0.19 and 0.57 µg/mL, respectively. The solubility of PR in PG, DMI, glycerol was within the range of 367 to 877 mg/mL. The stability of PR in tested solvents were also confirmed by the 72 h stability studies. From the DVS studies, 70-125% of applied formulations were recovered at 24h. The permeation through porcine skin at 24 h ranged from 4 to 13 µg/cm<sup>2</sup>, while the corresponding amounts of PR delivered through human skin were 2 to 10 µg/cm<sup>2</sup>.

#### CONCLUSION:

The physicochemical properties of PR confirm it is suitable for dermal delivery. In this study, propylene glycol was the most promising vehicle for PR delivery

to human skin. Future work will expand the range of vehicles studied and explore the percutaneous absorption from more complex formulations.

## Introduction

Melanin is the primary pigment responsible for the variation of colour observed in the skin, eye and hair of humans [1, 2]. Melanin is an aggregate of smaller nitrogenous molecules; it is produced within cell melanocytes located in basal layer of epidermis and transferred to keratinocytes throughout the epidermis [3, 4]. There are two types of melanin pigments found in human skin, the brown to black eumelanins and the red to yellow sulfur pheomelanins [5]. Skin darkness is directly related to the amount of eumelanin present, while melanocytes can produce varying ratios of eumelanin and pheomelanin in the process of melanogenesis [6]. It is believed that skin pigmentation has a photoprotective function; researchers have discovered that the two types of melanin appear to play different roles in this function [7]. Eumelanin serves as a physical barrier that scatters ultraviolet radiation (UVR) and as an absorbent filter that reduces the penetration of UV photons through the epidermis [8]. Pheomelanin shows weak photoprotective capability against UVR relative to eumelanin [9]. A deficiency in melanin can result in a series of dermatological problems, congenital hypopigmentation disorders including various types of oculocutaneous albinism and acquired hypopigmentation disorders such as vitiligo and Sutton nevus [10]. On the other hand, excess accumulation and uneven distribution of melanin is associated with dermatological conditions such as melasma [11]. Thus, developing safe and efficient treatments for unwanted skin pigmentation has attracted interest from both the cosmetic and pharmaceutical sectors [12].

Inhibitors of melanin synthesis and tyrosinase activity have been reviewed previously [6, 13–16]. Melanin is synthesized in the process of melanogenesis. Melanogenesis is a complex biosynthetic pathway involving a series of enzymatic catalyzed and chemical reactions. Three enzymes, tyrosinase, tyrosinase-related protein-1 (TRP-1), and tyrosinase-related protein-2 (TRP-2, also known as dopachrome tautomerase, DCT), play crucial roles in melanogenesis [6]. Initial melanin synthesis is catalyzed by tyrosinase, with the oxidation of L-tyrosine to dopaquinone (DQ) and /or L-dihydroxyphenylalanine (L-DOPA) to DQ which is the substrate for both eumelanin and pheomelanin synthesis (Fig. 1) [14]. Tyrosinase is a membrane-bound copper-containing glycoprotein (EC 1.14.18.1). At physiological pH, the remainder of the melanogenesis reaction sequence can spontaneously proceed, thus regulation of tyrosinase is a strategy for modulation of hyperpigmentation [16].

Phenylethyl resorcinol (PR, also known as 4-(1-phenylethyl)1,3-benzenediol) is a phenolic compound (Fig. 2) developed as a tyrosinase inhibitor [17, 18]. It inhibits tyrosinase activity and also demonstrated antioxidant benefits in cell culture studies [17, 19]. PR showed more than 20-fold efficiency in inhibition of mushroom tyrosinase compared with kojic acid. A concentration of 0.1% of PR resulted in almost complete suppression of melanin synthesis after 14 days application to pigmented 3D epidermis models [18]. An *in vivo* study examined the

efficacy of a formulation containing PR and other actives as an alternative to hydroquinone and kojic acid in 2012 [20]. After a 4-week washout period with a sunscreen, 20 female patients with mild-to-moderate melasma were treated with an oil-in-water emulsion cream containing disodium glycerophosphate, L-leucine, PR, and undecylenoyl phenylalanine for a 12-week period. The same daily sunscreen was consistently used during the treatment period. The facial skin of the patients was evaluated before and after the washout period and after the 12-week treatment period. There was no significant change in skin pigmentation during the 4-week washout; signs for uneven skin tone including appearance of lentigines and melasma area and severity index (MASI) decreased by up to 43% after the treatment. A later *in vivo* study investigated the same cream with a larger sample size [21]. The formulation was assessed for its effects on photoaging in 80 female subjects using visual assessment. After a 12-week application period, improvements in signs of facial skin discoloration were reported. However, there were significant limitations to this study, including the lack of a control group and evaluation of changes in pigmentation with subjective measurements. More recently, a number of publications have focused on the formulation of advanced carriers containing PR [22-24]. Fan and colleagues developed PR loaded nanostructured lipid carriers (PR-NLC) using a high-pressure homogenization approach [24]. Limsuwan and colleagues [23] designed Ethosome formulations containing 0.5% (w/v) PR, 0.5 % (w/v) cholesterol, 3% (w/v) L- $\alpha$ -phosphatidylcholine, 30% (v/v) absolute ethanol, and water up to 100% (v/v); the *in vitro* permeation of PR was subsequently evaluated using newborn pig skin with a application of 1 mL of 0.5 mg/mL PR-Ethosome formulation. At 24 h, the cumulative permeated amount of PR through skin was 58.7  $\mu\text{g}/\text{cm}^2$ . This appears to be the first study that investigated the permeation behaviour of PR *in vitro*. However, the experiment was conducted under infinite dose conditions and does not simulate typical amounts of a topical formulation that consumers apply to skin [25, 26]. Recently, Kang and Park [27] probed the mechanism of the anti-melanogenic activity of PR via a series of *in vitro* assays including assessment of cell survival, melanin content, cellular tyrosinase activity, real-time PCR analysis, luciferase-reporter assay, Western blot analysis, and ELISA assay of cyclic AMP (cAMP), protein kinase A (PKA), cAMP response element binding (CREB) protein, and mitogen-activated protein kinases (MAPKs). These authors reported that PR can attenuate melanogenesis by activating p44/42 MAPK which is a kinase that regulates signaling pathways mediating melanogenesis in melanocytes.

Despite these reported *in vitro* and *in vivo* studies of the biological effects of PR, there is little information in the literature with reference to the physicochemical properties of this compound. Therefore, the primary objective of this study was to undertake a comprehensive characterization of PR. As the skin penetration and delivery of PR to the skin is also not well understood, or documented, a secondary objective of the present work was to examine delivery of the molecule to mammalian skin from a range of solvents and permeation enhancers

widely used in personal care products.

## **Materials and methods**

### **Materials**

Phenylethyl resorcinol (Symrise, Holzminden, Germany) was a gift from pION Inc. Billerica, USA. Methanol, propylene glycol (PG) and glycerol were purchased from Fisher Scientific, UK. Dimethyl isosorbide (DMI) was kindly donated by Croda Ltd. (Goole, UK). Porcine tissue was supplied by a local abattoir. Excised abdominal human tissue was obtained from the UK Human Tissue Bank with appropriate institutional and ethical approval.

### **Nuclear Magnetic Resonance (NMR)**

<sup>1</sup>H NMR and <sup>13</sup>C NMR were recorded using a Bruker DMX-500 spectrometer operating at 500 MHz for proton and 126 MHz for carbon. Chemical shifts ( $\delta_H$  and  $\delta_C$ ) are quoted as parts per million downfield from 0. The multiplicity of <sup>1</sup>H NMR signals are designated by one of the following abbreviations: s = singlet, d = doublet, t = triplet, q = quartet and m = multiplet, and coupling constants (J) are expressed in Hertz. All data was processed using MestReNova® 9.0.1 (Mestrelab Research, Spain). PR was dissolved in Chloroform-d (CDCl<sub>3</sub>).

### **Thermal analysis**

The melting point of PR was examined using thermogravimetric analysis (TGA, TA Instruments, U.S.A.) and differential scanning calorimetry (DSC, TA instruments, USA). A suitable amount of PR was weighed in an open aluminium pan (TA Instruments, U.S.A.) and then heated inside the TGA furnace. The mass change of PR as a function of temperature increase was recorded. The initial temperature and the terminal temperature were set to 40 and 400 ° C with a heating ramp of 20 ° C/min. A nitrogen flow of 25 mL/min was supplied throughout the experiment to maintain an inert environment around the sample. To conduct DSC analysis, PR was weighed in a hermetic aluminium pan (TA Instruments, U.S.A.) and then subsequently sealed with a hermetic aluminium lid (TA Instruments, U.S.A.) using a Tzero™ press (TA Instruments, U.S.A.). The PR sample was heated from 0 to 150 ° C at 10 ° C/min under nitrogen (50 mL/min) supplement throughout the measurement. TA Universal software was used for data analysis.

### **Dynamic vapour sorption studies and preparation of PR solutions**

To study the evaporation or hydration of the vehicles, a Q5000 SA sorption analyzer (TA Instruments, U.S.A.) was used to examine the mass differences over 24 h. Nitrogen was used as the carrier gas at a flow rate at 200 mL/min. Temperature and relative humidity (RH) were maintained throughout the experiment at 32 ± 1° C and 50 ± 2% RH, respectively. Solutions of PR (1% w/v) were prepared in PG, DMI and glycerol.

### **UV, HPLC analysis and method validation**

To identify the wavelength number at which the absorption of light was selective for PR, a spectronic BioMate™ 3 UV/vis spectrophotometer (Thermo Scientific, U.S.A.) was used to conduct an UV scan of a solution of the active between 200 and 300 nm (step=1 nm). PR quantification was conducted using a HPLC (Agilent 1100, Agilent technologies, U.S.A., operated with ChemStation® Rev.A.09.03). The compound was analyzed with a Kinetix 5 µm C<sub>18</sub> 100 x 4.6 mm reverse phase column (Phenomenex, U.K.). The mobile phase consisted of methanol: water (60:40). The injection volume was set as 20 µL, the flow rate at 1 mL/min and the column temperature was 30 ° C. This method was validated according to guidelines established by the International Conference on Harmonisation of Technical Requirements for Registration of Pharmaceuticals for Human Use [28]. Linearity, specificity, accuracy, precision, lower limit of detection (LOD) and lower limit of quantification (LOQ) of the developed analytical methods were also determined.

#### **The logP (octanol water partition coefficient), solubility and stability determination**

The shake flask method was used to determine the partition coefficient of PR [29]. Octanol pre-saturated with water and water pre-saturated with octanol was prepared by mixing water and octanol in two stock bottles, one containing 100 mL octanol and a sufficient quantity of water, and the other containing 100 mL of water and a sufficient quantity of octanol. After stirring for 24 h at room temperature, 21° C , and equilibration for 48 h, the phases were separated. A stock solution of 100 mg/mL of PR in the saturated octanol layer was prepared. Three saturated octanol solutions of PR were prepared at 1 mg/mL with three different ratios of octanol: water (1:1, 1:2, 2:1). Vessels were agitated for 5 min, and the aqueous and organic phases were separated after 48 h. A sample from each phase was diluted and analysed by HPLC to calculate the log P as shown in Equation (1), where C<sub>octanol</sub> is the concentration of PR in the organic phase and C<sub>aqueous</sub> is the concentration in the aqueous phase. All measurements were conducted in triplicate.

$$\log P = \log \left( \frac{C_{\text{octanol}}}{C_{\text{aqueous}}} \right) \quad (1)$$

The solubility of PR in a series of vehicles was estimated by adding an excess amount of active into screw-cap glass vials containing a fixed amount of vehicle (2 mL, n=3). These vials were sealed with Parafilm® and placed in a water bath at 32±1 ° C for 48 h. A series of solvents including propylene glycol (PG), dimethyl isosorbide (DMI), and glycerol were selected for solubility determinations. The solubility of PR in PBS solution was also evaluated. The short-term stability of PR in the selected vehicles was examined over 72 h at 32±1 ° C. PR solutions were prepared at a concentration of 1 % (w/v) and the samples were analyzed by HPLC at time zero and at 24 h intervals up to 72 h.

### ***In vitro* permeation studies and mass balance studies**

The *in vitro* permeation studies of PR were conducted using vertical glass Franz diffusion cells as reported elsewhere [25, 30]. 1 % (w/v) solutions of PR in three vehicles, namely PG, DMI and glycerol, were prepared. The permeation was initially performed under finite dose conditions ( $5 \mu\text{L}/\text{cm}^2$ ) using full thickness porcine ear skin [31]. Subsequently the permeation behaviour was investigated using heat separated human epidermal membranes under the same dosing conditions. Porcine tissue was obtained from a local abattoir. Full-thickness skin was surgically removed from cartilage using scalpel as described by Caon et al [32]. Human epidermal membranes were prepared by heat separation as described previously [33]. Heat separation of porcine skin was not carried out as it has been shown to compromise the membrane integrity. Skin samples were stored at  $-20 \text{ }^\circ\text{C}$  until required. Skin integrity was examined by electrical resistance assessment before use [31]. Approximately 2 mL freshly prepared PBS solution ( $\text{pH } 7.3 \pm 0.1$ ) was used as the receptor medium and solubility determination confirmed that sink conditions were maintained throughout the experiments [34]. Franz cells were placed in a thermostatically controlled water bath (JB Nova, Grant, UK) set at  $36 \pm 1 \text{ }^\circ\text{C}$  and the temperature of the membrane was measured routinely until it equilibrated at  $32 \pm 1 \text{ }^\circ\text{C}$  (TM-22 Digitron digital thermometer, RS Components, Corby, UK).  $5 \mu\text{L}/\text{cm}^2$  of PR solutions were added into the donor chamber when the skin surface had equilibrated. Permeation studies were conducted up to 24 h. 200  $\mu\text{L}$  of receptor medium was withdrawn at each sampling interval (2, 4, 6, 8, 10, 12 and 24 h) and a same volume of fresh PBS solution was added to maintain a constant volume. All samples were analysed by HPLC.

Mass balance studies were conducted to examine the distribution of the active and to determine the total recovery [35]. The receptor medium was removed immediately once the permeation studies were complete. The skin surface was washed by adding 1 mL of water: methanol (10:90) three times for the  $5 \mu\text{L}/\text{cm}^2$  application. For each washing, the washing solution was transferred into an Eppendorf® tube. A cotton bud was used to swab the skin surface and the cotton bud was placed in Eppendorf® tubes with 1 mL of water: methanol (10:90). To extract PR contained in the skin, skin was removed from the Franz cells and cut into small pieces. These skin pieces were collected and put in Eppendorf® tubes with 1 mL of water: methanol (10:90). The Eppendorf® tubes were placed in an orbital shaker overnight at room temperature. Samples for skin extraction measurement were centrifuged at 13,200 rpm at room temperature for 20 min and all other samples were centrifuged at 12,000 rpm for 13 min. The supernatant solution was analyzed by HPLC. The mass balance approach was validated in advance of the study (data not shown). Results were calculated using Equation 2, where T is total recovery, W represents the recovery from the skin surface by washing and swabbing using the cotton bud, E is the value for skin extraction and P is the recovery from the receptor medium.

$$T = W + E + P \quad (2)$$

### Statistical analysis

Data were plotted using Microsoft® Excel. The statistical analysis was conducted using SPSS® Statistics Version 24 (IBM, USA). The data were examined for normality using the Shapiro-Wilk Test, and the homogeneity of variance was assessed using Levene's test. For data that meet the assumptions of normality and homogeneity of variance, one-way ANOVA was performed. Tukey's HSD post hoc test was used after ANOVA analysis to perform pairwise analysis. For non-parametric data or where the assumption of homogeneity of variance between groups was violated in the ANOVA analysis, the Kruskal-Wallis H test was used. A p-value lower than 0.05 ( $p < 0.05$ ) was considered a statistically significant difference. All the results are presented as mean  $\pm$  standard deviation.

### Results and discussion

#### NMR

The  $^1\text{H}$  and  $^{13}\text{C}$  NMR spectrums of PR in chloroform- $d$  are shown in Fig. 3. The structure was assigned and confirmed as follows:  $^1\text{H}$  NMR (500 MHz,  $\text{CDCl}_3$ )  $\delta$  7.35 - 7.30 (m, 2H, Ar-CH), 7.28 - 7.21 (m, 3H, Ar-CH), 7.12 (d,  $J = 8.3$  Hz, 1H, Ar-CH), 6.45 (dd,  $J = 8.3, 2.6$  Hz, 1H, Ar-CH), 6.32 (d,  $J = 2.5$  Hz, 1H, Ar-CH), 4.64 (s, 1H, OH), 4.63 (s, 1H, OH), 4.27 (q,  $J = 7.2$  Hz, 1H,  $\text{CH}_3\text{-CH}$ ), 1.62 (d,  $J = 7.2$  Hz, 3H,  $\text{CH}_3\text{-CH}$ );  $^{13}\text{C}$  NMR (126 MHz,  $\text{CDCl}_3$ )  $\delta$  155.10 (Quaternary-C), 154.34 (Quaternary-C), 145.47 (Quaternary-C), 128.78 (Aromatic-C), 128.63 (Aromatic-C), 127.41 (Aromatic-C), 126.54 (Aromatic-C), 124.31 (Quaternary-C), 107.62 (Aromatic-C), 103.54 (Aromatic-C), 38.39 (CH), 21.30 ( $\text{CH}_3$ ).

#### Thermal analysis

TGA measurement was conducted ahead of DVS investigation. There was no weight loss of PR up to 213.3 °C, which indicated the degradation occurs at 213.3 °C (Fig. 4). As shown in Fig. 5, the onset temperature of the melting point and the enthalpy of fusion were measured as 79.1 °C and 113.6 J/g, respectively. Furthermore, the purity of the PR sample was confirmed by the single endothermic event in the DSC curve in Fig. 5.

#### DVS results

Fig. 6 shows the DVS results for all PR solutions over 1440 min at  $32 \pm 1^\circ\text{C}$  and 50 % RH. Initially, an increase in weight was observed for all three tested solutions. This can be explained by the hygroscopic nature of PG, DMI and glycerol. The mass of PG and DMI solutions started to decrease at 67.2 and 43.1 min, respectively. The evaporation of PG was consistent with previous studies [36, 37]. The amounts of DMI, PG and glycerol vehicles remaining at 1440 min were  $69.5 \pm 2.4$ ,  $48.4 \pm 3.0$ , and  $124.0 \pm 1.6\%$ , respectively.



### **UV, HPLC analysis and method validation**

The detection wavelength for UV detection of PR was selected as 280 nm. For the HPLC analytical method validation, a calibration curve ranging from 0.25 to 50  $\mu\text{g/mL}$  was constructed. The correlation coefficient ( $r^2$ ) was 0.99 confirming the linearity of the method. The accuracy of this method was evaluated by spiking PR at three concentrations (1, 25, 50  $\mu\text{g/mL}$ ). The recovery rates within the range of 99.16 - 105.77% indicated this method was accurate for PR. The precision was evaluated by determination of inter-day variability and intra-day repeatability. The % relative standard deviation (RSD) values of intra-day variability studies were  $< 1.50\%$ ; while the % RSD results of inter-day precision were  $< 1.15\%$ . Based on the standard deviation and slope determination strategy, the limit of detection and limit of quantification were 0.19 and 0.57  $\mu\text{g/mL}$ , respectively.

### **logP (octanol water partition coefficient), solubility and stability determinations**

The mean value of the log P for the three octanol:water ratios evaluated was determined to be  $3.35 \pm 0.03$  at room temperature ( $21^\circ\text{C}$ ). This experimental value is in line with the predicted logP values. DrugBank published the calculated logP for PR as 3.74 and 3.02 using ChemAxon and ALOGPS, respectively [38]. Table I shows the results for the solubility studies. The solubility of PR in DMI, PG, glycerol was determined to be 877.1, 568.0 and 367.8  $\text{mg/mL}$ . The solubility of PR in PBS solution was determined as 3.4  $\text{mg/mL}$ . This confirmed that sink conditions would be maintained over the course of the permeation study. A concentration of 1% of PR in DMI, PG, or glycerol was selected as this within the range of the concentration found in the marketed products [39]. The stability of PR in DMI, PG, and glycerol was also evaluated at  $32 \pm 1^\circ\text{C}$ . After 72h, the recovery values of PR were  $> 93.0\%$ . The stability of PR in PBS solutions was also confirmed (Fig. 7).

### **Permeation studies**

The permeation behaviour of PR was investigated using both full thickness porcine skin with a comparable thickness of  $1.45 \pm 0.40\text{ mm}$  and heat separated human epidermal membranes under finite dose conditions. Permeation profiles of PR in pig skin are illustrated in Fig. 8A. Permeation of PR was evident from 8 h for DMI, however the permeation of PR was not detected for PG and glycerol solutions until 12h. The cumulative amounts of PR that permeated from DMI and PG at 24 h were  $12.9 \pm 1.7$  and  $11.0 \pm 6.3\ \mu\text{g/cm}^2$ , respectively ( $p > 0.05$ ). A significantly lower amount of PR was delivered from glycerol ( $4.3 \pm 2.1\ \mu\text{g/cm}^2$ ) compared with DMI ( $p < 0.05$ ).

Results for the mass balance studies are summarized in Table II. The recovery of PR from pig skin surface for PG and glycerol were  $17.8 \pm 7.3$  and  $17.3 \pm 5.4\%$ , respectively ( $p > 0.05$ ). Comparing to PG and glycerol, a lower recovery from the skin surface was evident for DMI solution, at  $2.6 \pm 1.3\%$  ( $p < 0.05$ ). The results

also confirmed that more than 70% of the applied doses of PR were delivered into porcine skin at 24 h for three tested solutions. The amounts of PR extracted from pig skin after the permeation study accounted for  $57.7 \pm 7.9$ ,  $53.8 \pm 9.1$  and  $48.9 \pm 8.1$  % of applied PR for PG, DMI and glycerol solutions, respectively. There is no significant difference among these values ( $p > 0.05$ ).

With reference to permeation studies conducted in human skin the PG solutions were more effective than DMI and glycerol solutions (Fig. 8B). Permeation of PR was detected from PG at 6 h. The cumulative permeation of PR from PG at 24 h was  $10.2 \pm 3.1$   $\mu\text{g}/\text{cm}^2$ . This value was significantly higher than DMI ( $9.1 \pm 2.3$   $\mu\text{g}/\text{cm}^2$ ) and glycerol ( $2.5 \pm 0.2$   $\mu\text{g}/\text{cm}^2$ ) solutions ( $p < 0.05$ ).

Table II summarized the results of mass balance studies. 22% of the applied dose of PR permeated through the epidermis for the PG solution. PG is the most commonly used glycol in transdermal and topical formulations, and it may act as a co-solvent and/or a permeation enhancer. Although the mechanism of PG penetration enhancement is not fully understood, it has been suggested that PG integrates into the polar regions of the lipids in the stratum corneum, disrupting the lamellar phase [40, 41]. DMI delivered 19 % of the applied dose of PR through human skin. DMI is a water-miscible liquid with a relatively low viscosity; it has also exhibited potential as a good solvent for non-polar molecules [42]. The permeation enhancement of DMI was also observed in skin delivery of niacinamide [25]. Glycerol solutions delivered 5 % of the applied PR through human skin ( $p > 0.05$ ). Unlike the permeation behavior observed in pig skin, a high percentage of PR was recovered from the human epidermal surface (Table II). The differences between the recovered percentages from human and pig skin surfaces were statistically significant for DMI and glycerol ( $p < 0.05$ ). The amount of PR extracted from porcine skin membrane was higher than the human skin retention for three tested solutions ( $p < 0.05$ ). For glycerol, 78% of the applied amount of PR remained on the skin surface, and 9% of the applied dose was extracted from human epidermis. Results for skin extraction of PR for DMI and PG indicated that 34 and 12% of the applied doses were retained within skin, respectively ( $p > 0.05$ ). For all tested solutions, the total recovery of PR was  $> 90\%$ . This was within the acceptable range of the relevant OECD guidelines [35]

For the three tested PR solutions, the cumulative permeated amount through full thickness porcine skin was within the range of 4 to 13  $\mu\text{g}/\text{cm}^2$ , while the corresponding amount in human skin ranged from 2 to 10  $\mu\text{g}/\text{cm}^2$ . When compare PR permeation in two models, the difference was only evident for DMI solution, a higher permeation in porcine skin (13  $\mu\text{g}/\text{cm}^2$ ) than human skin (9  $\mu\text{g}/\text{cm}^2$ ) ( $p < 0.05$ ). In human skin studies, for three tested solutions, more than 45% of applied PR was recovered from the skin surface. Significant differences were evident for the surface recovered percentages between DMI and glycerol solutions ( $p < 0.05$ ). The skin extraction values between all three tested vehicles were different

( $p < 0.05$ ), ranged from 9 to 34% of dosed amounts. The higher amounts found on the surface in the human skin studies warrants further investigation. If these amounts can be reduced by judicious formulation, more effective products that deliver actives into the skin can be produced.

The lower permeability of human skin compared with porcine skin is in line with findings reported by other researchers [25, 36, 43, 44]. However, the differences between PR permeated through human epidermis and pig skin were not statistically significant for PG and glycerol solutions ( $p > 0.05$ ). The pig skin used in this study included epidermal and dermal layers. For human skin, only heat separated epidermis was used. The hydrated dermal layer in full thickness porcine skin may be expected to act as an additional aqueous barrier for PR permeation [43]. This could explain the higher skin retention observed in porcine skin compared to human skin ( $P < 0.05$ ). The higher retention in pig skin membrane was also consistent with the results reported by others [36]. From the results obtained in this study, the permeability of human and porcine skin clearly is dependent on the molecule of interest. Human skin remains the “gold-standard” to evaluate the skin delivery of chemicals for transdermal and topical purposes researchers [45]. However, porcine skin, whilst not a perfect model to predict human skin permeation is a suitable model to assess PR mammalian skin permeation before progressing to studies in human skin [43, 46, 47].

## Conclusions

The characterization of the physicochemical properties of an active ingredient provides valuable information for development of a topical preparation of the material. To our knowledge this is the first study that reports a systematic characterization of PR. A new HPLC analytical method for the quantification of PR was developed and validated. The solubility and short-term stability of PR were investigated in varied solvents. Thermal analysis confirmed the melting point of PR as 79.1 ° C. The permeation of PR was also investigated in porcine and human skin under finite dose conditions. The permeation behavior of PR observed in both human and porcine skin from three tested solution were consistent with the physicochemical properties for its skin penetration, namely the  $< 300$  Da, melting point  $< 100$  ° C, and a favourable partition coefficient. Considering the application of this active, skin retention of PR rather than skin permeation into the deeper tissue is desirable. Further study is required to examine more complex formulations with combinations of solvents to probe how skin delivery of PR may be further optimised.

## References

1. Rzepka, Z., Buszman, E., Beberok, A. and Wrzeźniok, D. From tyrosine to melanin: signaling pathways and factors regulating melanogenesis. *Postepy higieny i medycyny doswiadczałnej (Online)*. 70:695-708 (2016).

2. Litwack, G. Chapter 13 – Metabolism of Amino Acids. In: *Human Biochemistry*. (G. Litwack, ed. eds), p. pp. 359–94. Academic Press, Boston (2018).
3. Jones, K., Hughes, J., Hong, M., Jia, Q. and Orndorff, S. Modulation of Melanogenesis by Aloesin: A Competitive Inhibitor of Tyrosinase. *Pigm Cell Res.* 15(5):335–40 (2002).
4. Merghoub, T., Polsky, D. and Houghton, A.N. Chapter 36 – Molecular Biology of Melanoma. In: *The Molecular Basis of Cancer (Third Edition)*. (J. Mendelsohn, P.M. Howley, M.A. Israel, J.W. Gray, C.B. Thompson, ed. eds), p. pp. 463–70. W.B. Saunders, Philadelphia (2008).
5. Kongshoj, B., Thorleifsson, A. and Wulf, H.C. Pheomelanin and eumelanin in human skin determined by high-performance liquid chromatography and its relation to in vivo reflectance measurements. *Photodermatol Photoimmunol Photomed.* 22(3):141–7 (2006).
6. Pillaiyar, T., Manickam, M. and Jung, S.-H. Recent development of signaling pathways inhibitors of melanogenesis. *Cell Signal.* 40:99–115 (2017).
7. Brenner, M. and Hearing, V.J. The protective role of melanin against UV damage in human skin. *Photochem Photobiol.* 84(3):539–49 (2008).
8. Hoogduijn, M.J., Cemeli, E., Ross, K., Anderson, D., Thody, A.J. and Wood, J.M. Melanin protects melanocytes and keratinocytes against H<sub>2</sub>O<sub>2</sub>-induced DNA strand breaks through its ability to bind Ca<sup>2+</sup>. *Exp Cell Res.* 294(1):60–7 (2004).
9. Mitra, D., Luo, X., Morgan, A., Wang, J., Hoang, M.P., Lo, J., et al. An ultraviolet-radiation-independent pathway to melanoma carcinogenesis in the red hair/fair skin background. *Nature.* 491:449 (2012).
10. Yamaguchi, Y. and Hearing, V.J. Melanocytes and their diseases. *Cold Spring Harbor perspectives in medicine.* 4(5):a017046 (2014).
11. Ryu, J.H., Seok, J.K., An, S.M., Baek, J.H., Koh, J.S. and Boo, Y.C. A study of the human skin-whitening effects of resveratryl triacetate. *Arch Dermatol Res.* 307(3):239–47 (2015).
12. Pillaiyar, T., Manickam, M. and Namasivayam, V. Skin whitening agents: medicinal chemistry perspective of tyrosinase inhibitors. *J Enzyme Inhib Med Chem.* 32(1):403–25 (2017).
13. Mishima, Y., Hatta, S., Ohyama, Y. and Inazu, M. Induction of Melanogenesis Suppression: Cellular Pharmacology and Mode of Differential Action. *Pigm Cell Res.* 1(6):367–74 (1988).
14. Ando, H., Kondoh, H., Ichihashi, M. and Hearing, V.J. Approaches to Identify Inhibitors of Melanin Biosynthesis via the Quality Control of Tyrosinase. *J Invest Dermatol.* 127(4):751–61 (2007).
15. Mishima, Y. and Kondoh, H. Dual Control of Melanogenesis and Melanoma Growth: Overview: Molecular to Clinical Level and the Reverse. *Pigm Cell Res.* 13:10–22 (2000).
16. Olivares, C. and Solano, F. New insights into the active site structure and catalytic mechanism of tyrosinase and its related proteins. *Pigment Cell Melanoma Res.* 22(6):750–60 (2009).
17. Sorg, O., Kasraee, B., Salomon, D. and Saurat, J.H. The Combination of a Retinoid, a Phenolic Agent and an Antioxidant Improves Tolerance while Retaining an Optimal

- Depigmenting Action in Reconstructed Epidermis. *Dermatology*. 227(2):150–6 (2013).
18. Vielhaber, G., Schmaus, G., Jacobs, K., Franke, H., Lange, S., Herrmann, M., et al. 4 - (1 - Phenylethyl) 1, 3 - Benzenediol: A New, Highly Efficient Lightening Agent. *Int J Cosmet Sci*. 29(1):65–6 (2007).
  19. Linder, J. Topical melasma treatments. *Pigmentary Disorders*. 1(115):1–3 (2014).
  20. Gold, M.H. and Biron, J. Efficacy of a novel hydroquinone - free skin - brightening cream in patients with melasma. *J Cosmet Dermatol*. 10(3):189–96 (2011).
  21. Dreher, F., Draelos, Z.D., Gold, M.H., Goldman, M.P., Fabi, S.G. and Puissegur Lupo, M.L. Efficacy of hydroquinone - free skin - lightening cream for photoaging. *J Cosmet Dermatol*. 12(1):12–7 (2013).
  22. Amnuakit, T., Limsuwan, T., Khongkow, P. and Boonme, P. Vesicular carriers containing phenylethyl resorcinol for topical delivery system; liposomes, transfersomes and invasomes. *Asian J Pharm Sci*. (2018).
  23. Limsuwan, T., Boonme, P., Khongkow, P. and Amnuakit, T. Ethosomes of Phenylethyl Resorcinol as Vesicular Delivery System for Skin Lightening Applications. *Biomed research international*. 2017 (2017).
  24. Fan, H., Liu, G., Huang, Y., Li, Y. and Xia, Q. Development of a nanostructured lipid carrier formulation for increasing photo-stability and water solubility of Phenylethyl Resorcinol. *Appl Surf Sci*. 288:193–200 (2014).
  25. Zhang, Y., Lane, M.E., Hadgraft, J., Heinrich, M., Chen, T., Lian, G., et al. A comparison of the in vitro permeation of niacinamide in mammalian skin and in the Parallel Artificial Membrane Permeation Assay (PAMPA) model. *Int J Pharm*. 556:142–9 (2019).
  26. Haque, T., Lane, M.E., Sil, B.C., Crowther, J.M. and Moore, D.J. In vitro permeation and disposition of niacinamide in silicone and porcine skin of skin barrier-mimetic formulations. *Int J Pharm*. 520(1):158–62 (2017).
  27. Kang, M., Park, S.-H., Park, S.J., Oh, S.W., Yoo, J.A., Kwon, K., et al. p44/42 MAPK signaling is a prime target activated by phenylethyl resorcinol in its anti-melanogenic action. *Phytomedicine*. 58:152877 (2019).
  28. ICH. Validation of analytical procedures: text and methodology, 1–13. ICH, (2005).
  29. OECD. Test No. 107: Partition Coefficient (n-octanol/water): Shake Flask Method: OECD Publishing (1995).
  30. Santos, P., Watkinson, A.C., Hadgraft, J. and Lane, M.E. Oxybutynin permeation in skin: The influence of drug and solvent activity. *Int J Pharm*. 384(1):67–72 (2010).
  31. Oliveira, G., Hadgraft, J. and Lane, M.E. The influence of volatile solvents on transport across model membranes and human skin. *Int J Pharm*. 435(1):38–49 (2012).
  32. Caon, T., Costa, A.C., de Oliveira, M.A., Micke, G.A. and Simões, C.M. Evaluation of the transdermal permeation of different paraben combinations through a pig ear skin model. *Int J Pharm*. 391(1):1–6 (2010).
  33. Kligman, A.M. and Christophers, E. Preparation of isolated sheets of human stratum corneum. *Arch Dermatol*. 88(6):702–5 (1963).
  34. Pellett, M.A., Roberts, M.S. and Hadgraft, J. Supersaturated solutions evaluated with an in vitro stratum corneum tape stripping technique. *Int J Pharm*. 151(1):91–8 (1997).

35. OECD. Test No. 428: Skin Absorption: In Vitro Method: OECD Publishing (2004).
36. Paz-Alvarez, M., Pudney, P.D.A., Hadgraft, J. and Lane, M.E. Topical delivery of climbazole to mammalian skin. *Int J Pharm.* 549(1):317-24 (2018).
37. Haque, T., Rahman, K.M., Thurston, D.E., Hadgraft, J. and Lane, M.E. Topical delivery of anthramycin I. Influence of neat solvents. *Eur J Pharm Sci.* 104:188-95 (2017).
38. DrugBank. phenylethyl resorcinol. Available online: <https://www.drugbank.ca/drugs/DB14120> (15/07/2019).
39. Gohara, M., Yagami, A., Suzuki, K., Morita, Y., Sano, A., Iwata, Y., et al. Allergic contact dermatitis caused by phenylethyl resorcinol [4-(1-phenylethyl)-1,3-benzenediol], a skin-lightening agent in cosmetics. *Contact Dermatitis.* 69(5):319-20 (2013).
40. Lane, M.E. Skin penetration enhancers. *Int J Pharm.* 447(1):12-21 (2013).
41. Brinkmann, I. and Müller-Goymann, C. An attempt to clarify the influence of glycerol, propylene glycol, isopropyl myristate and a combination of propylene glycol and isopropyl myristate on human stratum corneum. *Pharmazie.* 60(3):215-20 (2005).
42. Zia, H., Ma, J.K.H., O'Donnell, J.P. and Luzzi, L.A. Cosolvency of Dimethyl Isosorbide for Steroid Solubility. *Pharm Res.* 8(4):502-4 (1991).
43. Dick, I.P. and Scott, R.C. Pig ear skin as an in-vitro model for human skin permeability. *J Pharm Pharmacol.* 44(8):640-5 (1992).
44. Singh, S., Zhao, K. and Singh, J. In vitro permeability and binding of hydrocarbons in pig ear and huamn abdominal skin. *Drug Chem Toxicol.* 25(1):83-92 (2002).
45. Franz, T.J. Percutaneous Absorption. On the Relevance of in Vitro Data. *J Invest Dermatol.* 64(3):190-5 (1975).
46. Barbero, A.M. and Fräsch, H.F. Pig and guinea pig skin as surrogates for human in vitro penetration studies: A quantitative review. *Toxicol In Vitro.* 23(1):1-13 (2009).
47. Yoshimatsu, H., Ishii, K., Konno, Y., Satsukawa, M. and Yamashita, S. Prediction of human percutaneous absorption from in vitro and in vivo animal experiments. *Int J Pharm.* 534(1-2):348-55 (2017).

Figure document

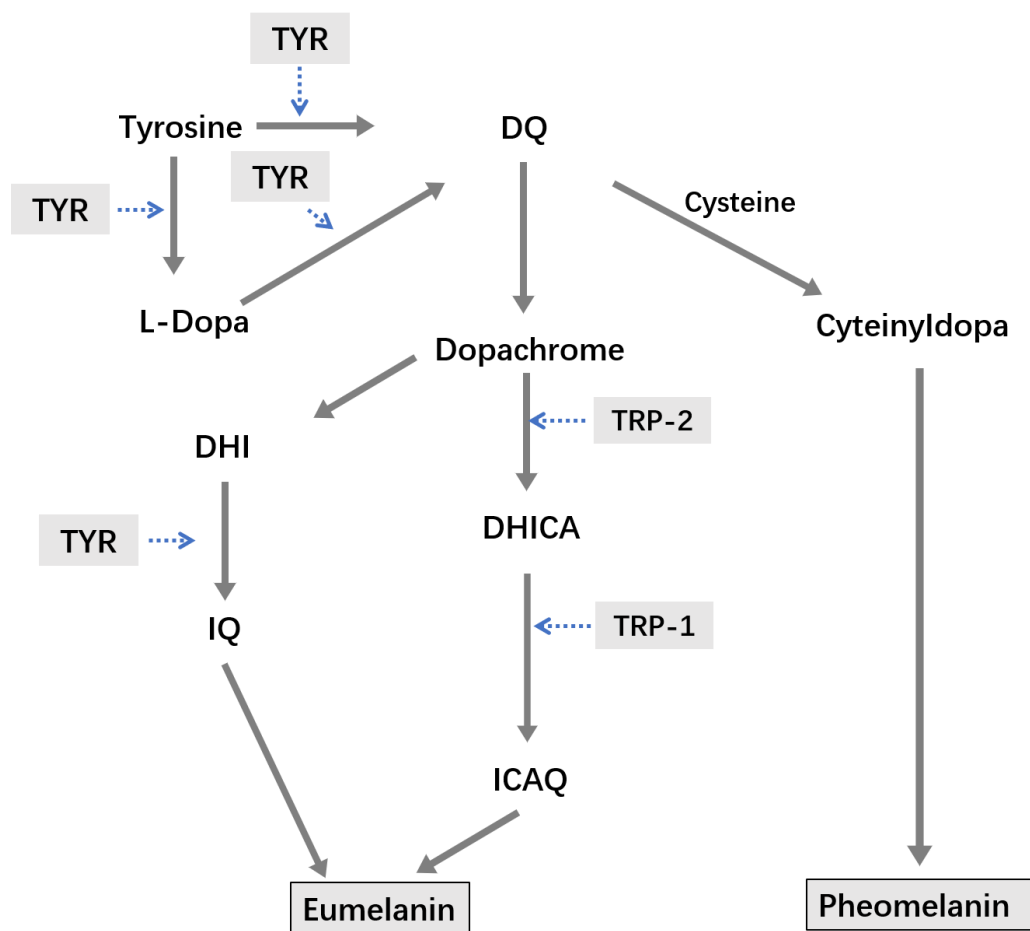


Figure 1. Biosynthetic pathway of melanin. Eumelanin and pheomelanin are synthesized with a series of reactions that are catalyzed by melanogenic enzymes. Hydroxylation of tyrosine to L-DOPA is the rate-limiting step catalyzed by tyrosinase; TRP-1 and TRP-2 are also involved in eumelanogenesis. This figure was adopted [14] and modified. (TYR, tyrosinase; DQ, dopaquinone; L-Dopa, L-3,4-dihydroxyphenylalanine; DHICA, 5,6-dihydroxyindole-2 carboxylic acid; DHI, 5,6-dihydroxyindole; ICAQ, indole-2-carboxylic acid-5,6-quinone; IQ, indole-5,6-quinone, TRP-1, tyrosinase-related protein 1; TRP-2, tyrosinase-related protein 2).

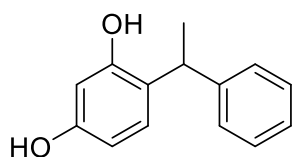
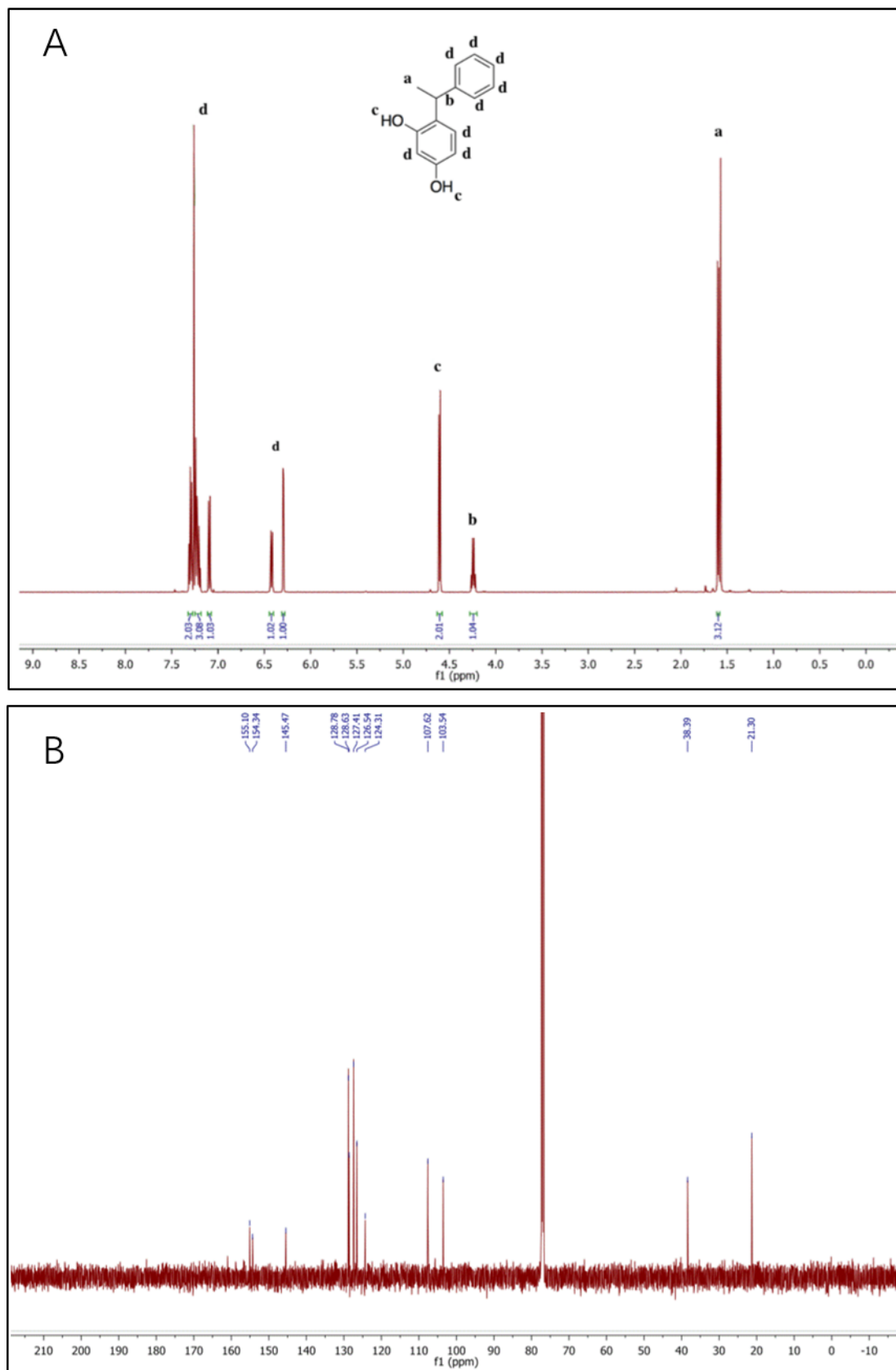


Figure 2. The 2D structure of phenylethyl resorcinol.





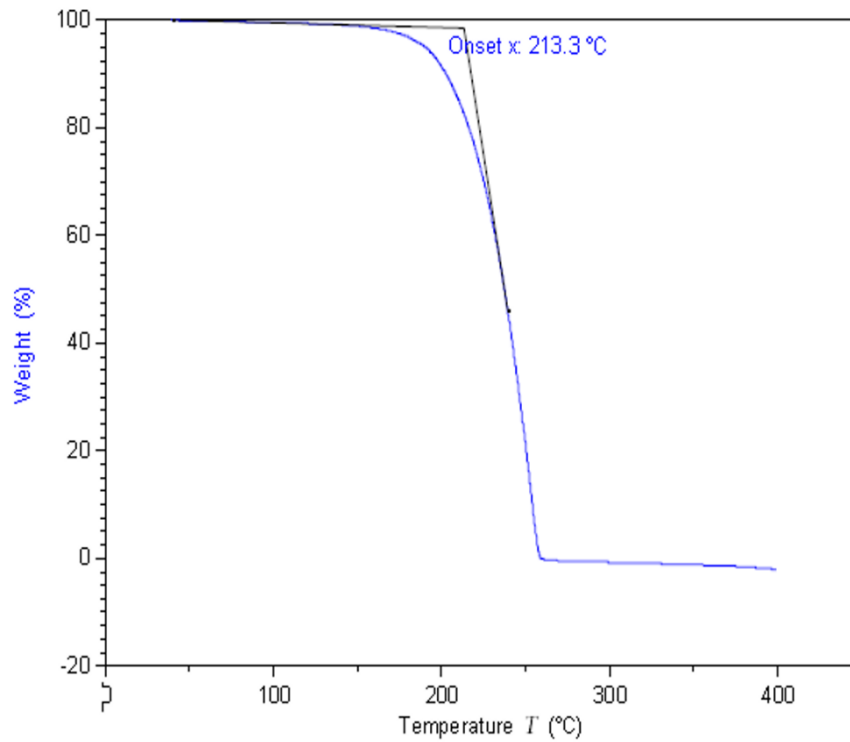


Figure 4. Thermogravimetric analysis (TGA) of PR from 40 to 400 °C with a heating ramp of 20 °C/min.

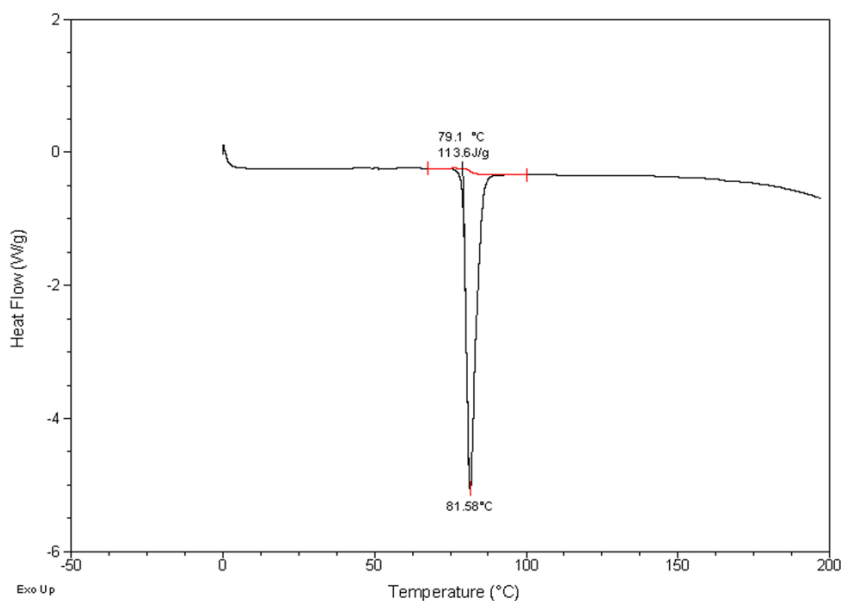


Figure 5. Differential scanning calorimetry (DSC) analysis of PR from 0 to 150 °C with a heating ramp of 10 °C/min.

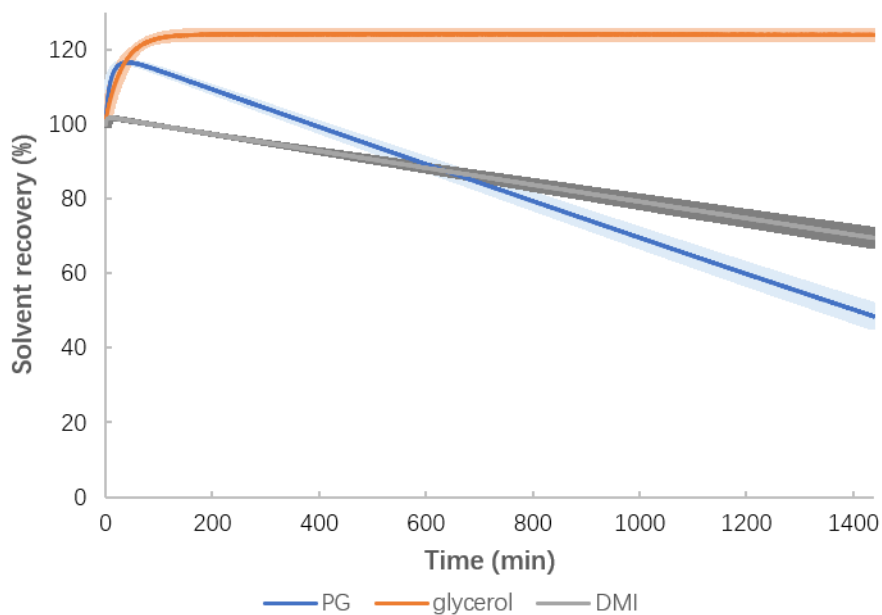


Figure 6. Percentage of weight loss over 1440 min from 1% PR solution in DMI, PG and Glycerol as prepared for human skin and porcine skin permeation studies. n=3, mean±SD.

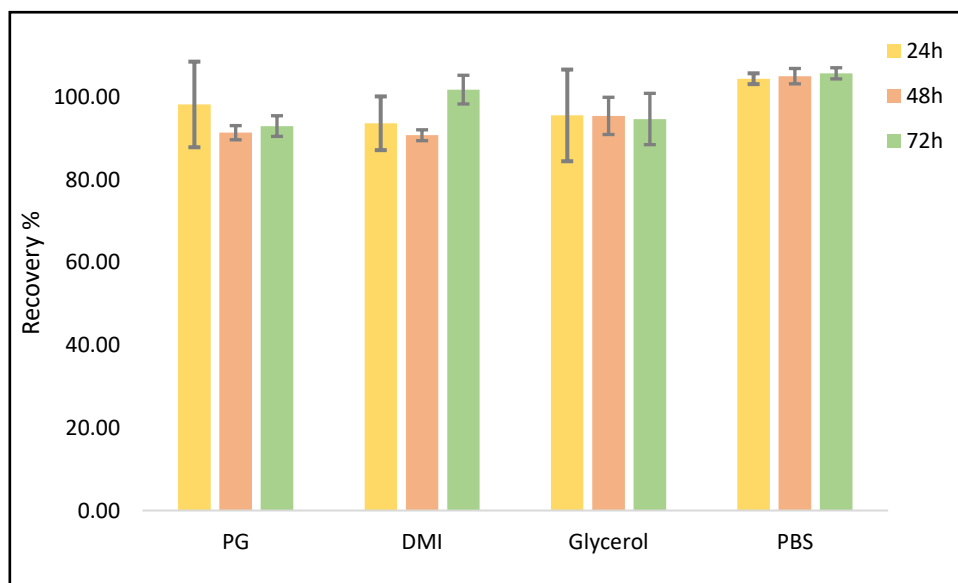


Figure 7. the results of the stability studies of PR in PG, DMI, glycerol, and the PBS solution for up to 72 h. n=3, mean±SD.

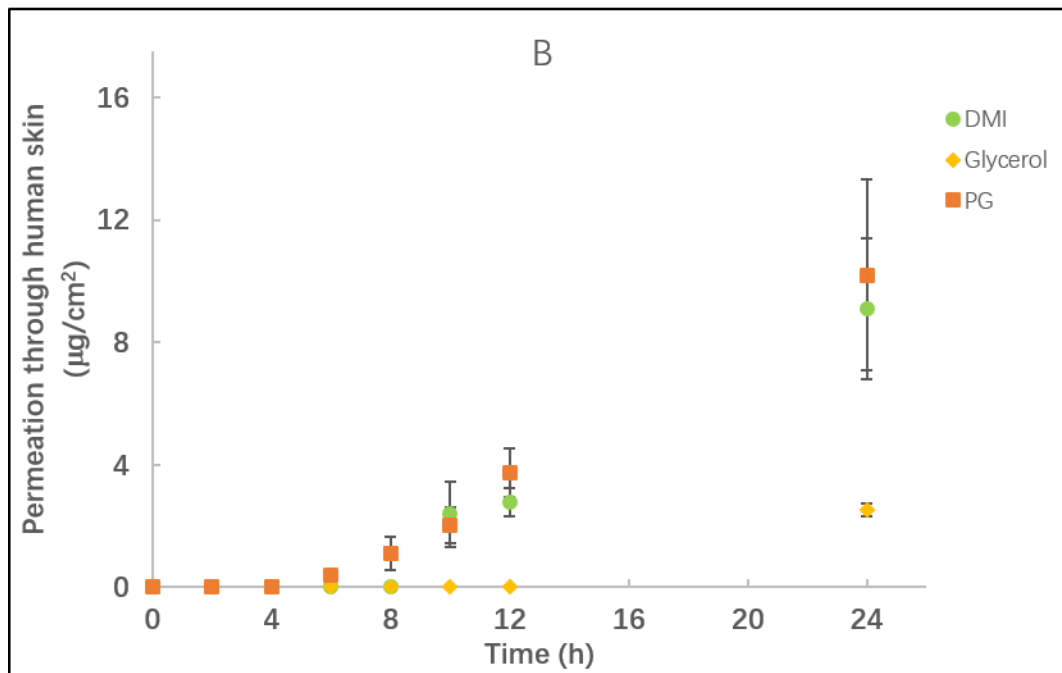
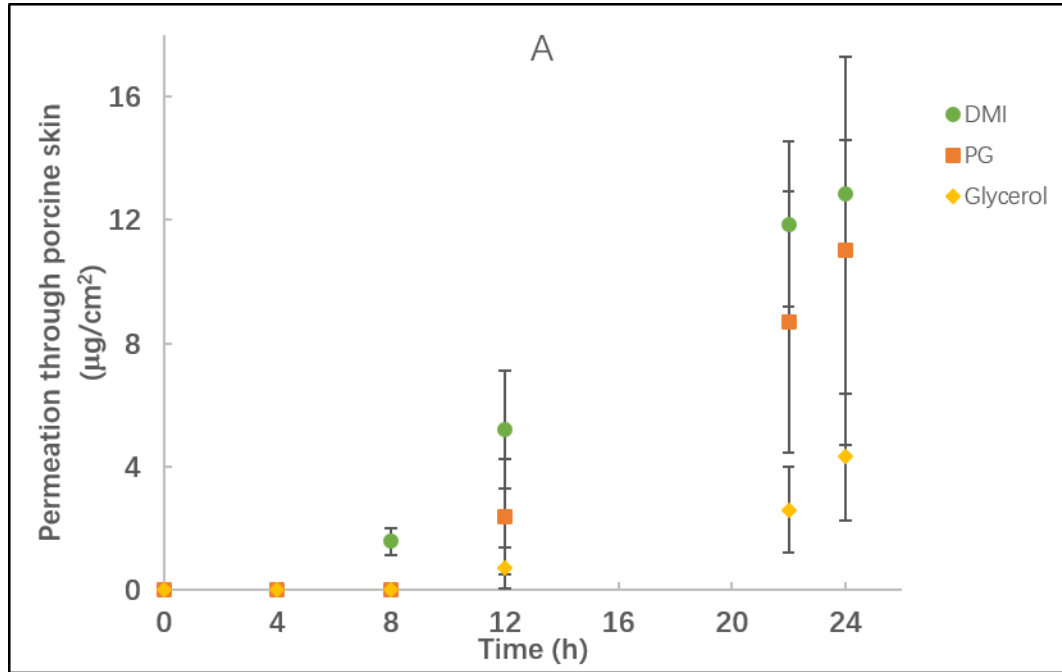


Figure 8. The permeation profiles of PR through porcine skin (A) and human skin (B) under finite dose application of 1% (w/v) PR in PG (■), DMI (●) and Glycerol (◆).  $4 \leq n \leq 5$ , mean  $\pm$  SD.

Table I. The solubility of PR in a series of vehicles, HPLC water and PBS solution (n=3, mean $\pm$ SD).

Solvent	Solubility of PR mg/mL
DMI	877.1 $\pm$ 14.2
PG	568.0 $\pm$ 3.5
Glycerol	367.8 $\pm$ 12.7
PBS	3.4 $\pm$ 0.1
water	3.7 $\pm$ 3.2